How to cite: *Angew. Chem. Int. Ed.* **2022,** *61,* e202207623
International Edition: doi.org/10.1002/anie.202207623
German Edition: doi.org/10.1002/ange.202207623

Helical Polymers

Photostability and Dynamic Helical Behavior in Chiral Poly(phenylacetylene)s with a Preferred Screw-Sense

*Francisco Rey-Tarrío, Santiago Guisán-Ceinos, Juan M. Cuerva, Delia Miguel, Maria Ribagorda, Emilio Quiñoá, and Félix Freire**

Abstract: Helical polymers such as poly(phenylacetylene)s (PPAs) are interesting materials due to the possibility of tuning their helical scaffold (sense and elongation) once they have been prepared and by the presence of external stimuli. The main limitation in the application of PPAs is their poor photostability. These polymers degrade under visible light exposure through a photochemical electrocyclization process. In this work, it was demonstrated, through a selected example, how the photochemical degradation in PPAs is directly related to their dynamic helical behavior. Thus, while PPAs with dynamic helical structures show poor photostability under UV/Vis light exposure, poly-(*R*)-**1**, bearing an enantiopure sulfoxide group as pendant group and designed to have a quasi-static helical behavior, shows a large photostability due to the restricted conformational composition at the polyene backbone, needed to orient the conjugated double bonds prior to the photochemical electrocyclization process and the subsequent degradation of the material.

Dynamic helical polymers such as poly(phenylacetylene)s (PPAs) have attracted the attention of the scientific community due to their stimuli responsive properties.[1–12] Thus, modulation of either the helical sense[13–19] and/or elongation[20–28] of a PPA is possible by using different external stimuli such as metal ions,[13,29,31,32] chiral molecules,[33] temperature,[34–36] solvents,[37–41] or anions.[42–44] However, the industrial application of these polymers as chiral stationary phases,[45,46] chiral recognition reagents,[47–50] or as dynamic chiral ligands in asymmetric synthesis[51,52] is reduced due to their poor thermal or light exposure stability.[53–57]

On the other hand, static helical polymers, although they do not show stimuli-responsive properties, have important applications in fields such as chiral recognition, chiral stationary phases, or chiral catalysts among others,[1] due to the robustness and folding degree of the helical scaffold that is not perturbed by environmental conditions. A great challenge for the scientific community is to create dynamic or static helical polymers using the same polymeric material, where the advantages of both, dynamic and static helical polymers can be compared.

Recently, our group found that the stability of PPAs under light exposure is directly related to the elongation degree of the polyene backbone,[58] which is defined by the dihedral angle between conjugated double bonds (ω_1). Thus, compressed *cis-cisoidal* PPAs ($\omega_1 < 90°$) show lower stability than extended *cis-transoidal* PPAs ($\omega_1 > 90°$). This fact makes possible not only to distinguish between compressed and extended helical structures but also to estimate a value for ω_1 in a PPA with unknown secondary structure. In addition, these studies also revealed that in extended almost planar structures ($\omega_1 > 170°$), the dynamic behavior of the PPAs is dramatically reduced due to their restricted conformational freedom at the pendant group caused by steric effects—e.g. ortho substituted PPAs—, resulting in a null isomerization of conjugated double bonds under light exposure.

In this work, we want to go a step forward and establish a relationship between the dynamic behavior of a PPA and its stability, which should be applied to all the PPA helical scaffolds and not only to the highly stretched ones ($\omega_1 >$

[*] F. Rey-Tarrío, E. Quiñoá, F. Freire
Centro Singular de Investigación en Química Biolóxica e Materiais Moleculares (CiQUS) and Departamento de Química Orgánica, Universidade de Santiago de Compostela
15782 Santiago de Compostela (Spain)
E-mail: felix.freire@usc.es

S. Guisán-Ceinos, M. Ribagorda
Departamento de Química Orgánica, Facultad de Ciencias, Universidad Autónoma de Madrid
28049 Madrid (Spain)

J. M. Cuerva
Departamento de Química Orgánica. Facultad de Ciencias, Universidad de Granada (UGR), Unidad de Excelencia de Química Aplicada a la Biomedicina y Medioambiente (UEQ)
18071 Granada (Spain)

D. Miguel
Departamento de Fisicoquímica. Facultad de Farmacia, Universidad de Granada (UGR, UEQ)
18071 Granada (Spain)

M. Ribagorda
Institute for Advanced Research in Chemical Sciences (IAdChem), Universidad Autónoma de Madrid
28049 Madrid (Spain)

170°). To do that, it is necessary to prepare a PPA that comprises two requirements: 1) a "quasi static" behavior and 2) a helical scaffold where the dihedral angle between conjugated double bonds is lower than 170° ($\omega_1 < 170°$), scaffolds that are known to be effectively affected by light when the PPA is dynamic. In such system (PPA with quasi-static behavior and $\omega_1 < 170°$), it should be possible to determine if the dynamic helical character of the PPA affects to its stability under light exposure. To create a PPA that comprises these two features, it is necessary to make a rational monomer design. Thus, we envisioned monomer mono-(*R*)-**1** as a potential candidate to generate a PPA that adopts a helical scaffold with a quasi-static behavior (Figure 1a). This sulfynilarene was previously used as source of chirality in *ortho*-phenylene ethynylene (*o*-OPE) foldamers, allowing an efficient transfer of chirality to the helically folded *o*-OPE, leading to electronic circular dichroism (ECD), circularly polarized luminescence (CPL)- and vibrational circular dichroism (VCD)-active compounds.[59–61]

Based in our expertise in the field of helical polymers and sulfinyl arenes, we foresee that polymerization of *para*-sulfynilaryl acetylene monomer (*R*)-**1** will generate a PPA that comprises the desired requirements, helical structure with $\omega_1 < 170°$ and quasi-static behavior. The chiral sulfoxide group present in **1** is a medium size pendant group and

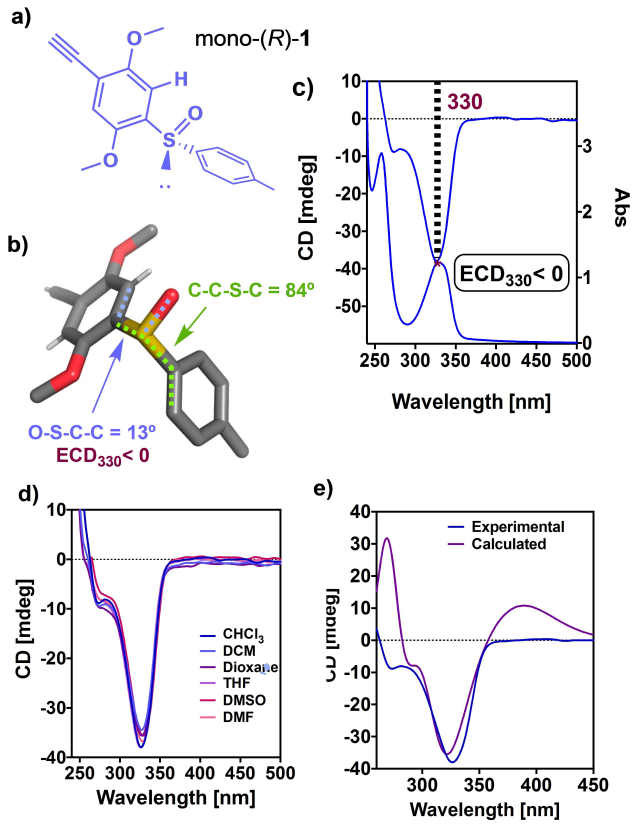

Figure 1. a) Chemical structure and b) X-ray of mono-(*R*)-**1**. c) Experimental ECD and UV spectra of mono-(*R*)-**1** in $CHCl_3$. [mono-(*R*)-**1**] = 0.3 mg mL^{-1}. d) Experimental ECD and UV spectra of mono-(*R*)-**1** in different solvents ([mono-(*R*)-**1**] = 0.3 mg mL^{-1}). e) Comparison of calculated and experimental ECD spectra of mono-(*R*)-**1** in $CHCl_3$.

presents the ability to favor a single conformation, thanks to the vicinal disposition of the methoxy group,[62] fact that should enhance its power as helical inductor and promote the formation of a helical scaffold with a $\omega_1 < 170°$. Therefore, it is expected that the orientation of the chiral pendant group respect to the polyene along the helical scaffold will be the same, producing an effective transfer of chirality from the enantiopure sulfoxide used as pendant to the polyene backbone.

To test our hypothesis, monomer (*R*)-**1** was prepared accordingly to a previously reported method.[59,62] X-ray diffraction series (XRD) of mono-(*R*)-**1** crystals obtained from a chloroform solution showed the presence of a preferred conformer where the sulfoxide group is oriented towards the phenylacetylene group, placing the oxygen group oriented planar towards the H at *ortho* position of the aryl ring (O–S–C–C angle = 13°) (Figure 1b).[63]

Electronic circular dichroism studies of mono-(*R*)-**1** in different solvents reveal a restricted conformational composition, where the ECD trace is not affected by either the polarity or the donor character of the solvent (Figure 1d). Moreover, the *p*-tolyl group is arranged almost perpendicular to the plane formed by the phenylacetylene and the methoxy groups (C–C–S–C dihedral angle of 84°), avoiding the repulsions between methoxy and sulfoxide groups (Figure 1a), and generating a chiral distribution between planes, which results in a strong absorption on CD and UV/Vis around 330 nm (Figure 1c, d).

Theoretical ECD calculations, time-dependent density functional theory (TD-DFT) was used together with a rCAM-B3LYP density functional and 6-31G* basis set (TD-DFT(rCAM-B3LYP)/6-31G*), were performed on the molecular structure obtained from X-ray studies. The simulated ECD spectrum is in good agreement with the experimental one obtained in all the different solvents tested indicating that mono-(*R*)-**1** adopts, as expected, the same conformation in solution that in the solid state (Figure 1e).

Next, mono-(*R*)-**1** was polymerized using $[Rh(nbd)Cl]_2$ as catalyst (nbd = 2,5-norbornadiene), affording poly-(*R*)-**1** in good yield (66 %, Figure 2) and with a high content of *cis* configuration of the double bonds as inferred from ^{1}H NMR and Raman studies (see Supporting Information for experimental details and characterization data). The number-average molecular weight (M_n = 88701) and distribution (M_w/M_n = 2.15) of the oligomers were determined by gel permeation chromatography (GPC) using THF as eluent with polystyrene standards as calibrants (see Supporting Information).

ECD and UV studies of poly-(*R*)-**1** were carried out in different solvents with different polarity and donor character to determine if poly-(*R*)-**1** adopts a helical structure with a preferred helical sense and tunable scaffold (Figure 2). In all solvents tested an ECD trace with and intense negative Cotton in the less energetic band indicates an *M* helical orientation of the polyene backbone (Figure 2b, c). Moreover, comparison of the mono-(*R*)-**1** and poly-(*R*)-**1** ECD and UV spectra show that the Cotton bands of the monomers are preserved in the PPA where two consecutive negative Cotton bands at ca. 260 and 310 nm are present.

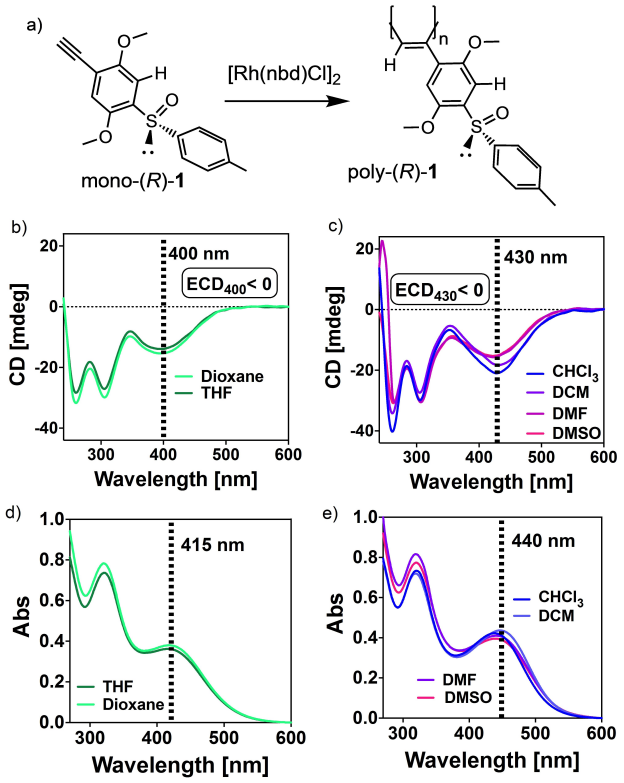

Figure 2. a) Polymerization scheme of mono-(*R*)-**1**. ECD spectra of poly-(*R*)-**1** in b) dioxane and THF or in c) DMF, DMSO, DCM and $CHCl_3$. UV/Vis spectra of poly-(*R*)-**1** in d) dioxane and THF or in e) DMF, DMSO, DCM and $CHCl_3$. [poly-(*R*)-**1**] = 0.3 mg mL^{-1}.

The hypsochromic shifting of the ECD band at 310 nm (330 in monomer) is due to the overlapping with other Cotton effects present in the polymer, such as the classical alternating −/+/− or +/−/+ Cotton bands usually found in PPAs.[64] Moreover, this overlapping of Cotton effect affects not only to the wavelength of the peaks but also to their intensity. In this case, the intensity of the Cotton bands related to the pendant group have similar intensity while in the monomer the UV band at 301 nm is four times the band at 260 nm.

Apart from these two bands, a new ECD/UV band appears at ca. 400 nm. ECD and UV/Vis experiments show that this band suffers a bathochromic shift of ca. 30 nm when is dissolved in DCM or $CHCl_3$ (430 nm) respect to the value obtained in THF or dioxane (400 nm) (Figure 2b,c). Therefore, the polymer adopts a more compressed helical scaffold ($ECD_{400} < 0$) in THF or Dioxane than when is dissolved in DCM, $CHCl_3$, DMF or DMSO ($ECD_{430} < 0$). Moreover, the absorbance of the yellowish polyene solution at wavelengths lower than 500 nm indicates that the poly(phenylacetylene) backbone does not adopt a highly extended, almost planar, helical scaffold, which usually shows a reddish color solution with a maximum of the polyene band at > 500 nm.[65,66]

To determine an approximated tridimensional structure for poly-(*R*)-**1** in $CHCl_3$ and THF, AFM studies were carried out. Thus, 2D crystals of poly-(*R*)-**1** were prepared following of Yashima's protocol which consist in spin coat a dilute solution of the polymer onto a highly oriented pyrolytic graphite (HOPG) substrate and leave the sample under solvent atmosphere for 12 h.[66] As a result, well-ordered 2D crystals of poly-(*R*)-**1** were obtained in both solvents, which allowed to obtain high-resolution AFM images for poly-(*R*)-**1** in $CHCl_3$ and THF. From these images is possible to extract important helical parameters such as the orientation of the helical structure described by the pendant groups or the helical pitch. In PPAs, the helical scaffold is defined by two coaxial helices. A helical structure is described by the polyene backbone, denoted as internal helix (H_{int}), whose helical sense can be determined by the sign of the Cotton bands associated to the polyene band—ECD < 0, M_{helix}; ECD > 0, P_{helix}—, and an external helix (H_{ext}) defined by the pendant groups whose orientation can be determined from AFM studies (Figure 3a,b).

As it was mentioned above, ECD studies showed that the internal helix of poly-(*R*)-**1** is oriented describing an *M* helix due to the presence of a negative Cotton band at ca. 400 nm in THF and at ca. 430 nm in $CHCl_3$. In addition, AFM images for poly-(*R*)-**1** in $CHCl_3$ revealed a right-handed orientation of the external helix, which is opposite to the orientation of the internal helix. These data correspond to a *cis-transoidal* polyene skeleton with $\omega_1 > 90°$. With the aim of refining the helical scaffold adopted by

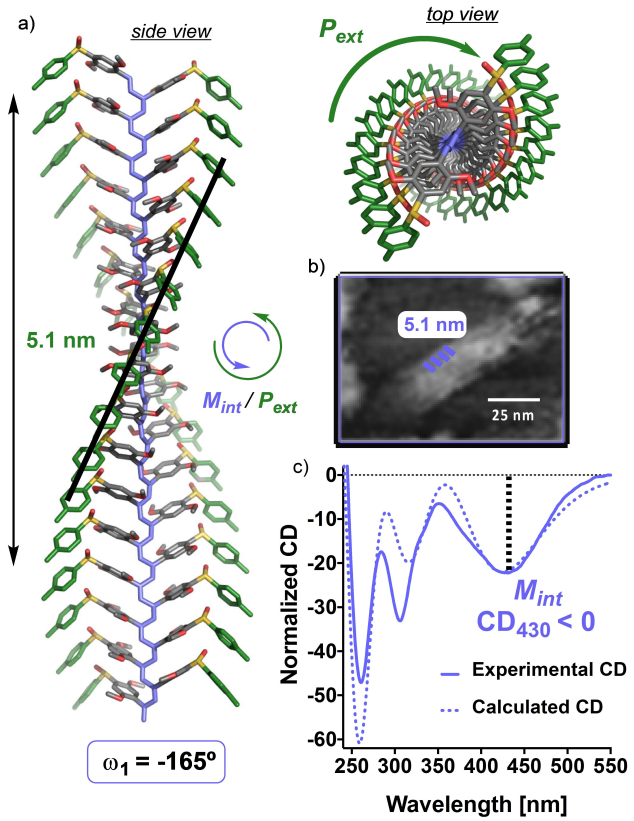

Figure 3. a) 3D structure adopted by poly-(*R*)-**1** in $CHCl_3$. b) AFM image of a 2D crystal of poly-(*R*)-**1** prepared in $CHCl_3$. c) Theoretical and experimental ECD spectra of poly-(*R*)-**1** (normalized at 430 nm). [poly-(*R*)-**1**] = 0.3 mg mL^{-1}.

poly-(*R*)-**1**, another helical parameter such as the helical pitch of ca. 5.1 nm, obtained from the AFM, was introduced into the modelling studies. The helical scaffold that satisfies the two structural data, $\omega_1 > 90°$ and helical pitch of ca. 5.1 nm, is a helix with $\omega_1 = -165°$.

Computational studies [TD-DFT(rCAM-B3LYP)/3-21G*] were performed on an *M* helix ($n = 8$) of poly-(*R*)-**1**-*cis-transoidal* skeleton ($\omega_1 = -165°$). In this model, the chiral moiety was introduced into the conformation obtained from X-ray studies. The simulated ECD spectrum is in good agreement with the one obtained experimentally, reproducing all the ECD bands and their relative intensity (Figure 3c).

On the other hand, AFM studies for poly-(*R*)-**1** in THF showed fiber like structures with a right-handed orientation of the external helix (Figure 4a). From these images it is not possible to extract helical parameters such as the helical pitch because bundled helical nanostructures rather than individual helices are visualized. Thus, to build up an approximated structure for poly-(*R*)-**1** in THF it was considered that the polyene scaffold is compressed when compared to the helix adopted in $CHCl_3$ ($\omega_1 = -165°$) due to the hypsochromic effect observed in the polyene band. Hence, molecular mechanics studies (MMFF94) were done to optimize the geometry of poly-(*R*)-**1** with $\omega_1 < -165°$, and where the calculated and the experimental ECD spectra show a good fit (Figure 4c). In this case, it was found that computational studies [TD-DFT(rCAM-B3LYP)/3-21G*] on an *M* helix ($n = 8$) of poly-(*R*)-**1** *cis-transoidal* skeleton, with a dihedral angle between conjugated double bonds of $\omega_1 = -157°$, produces a ECD trace that shows a good fit with the experimental one.

Finally, photostability studies were carried out for both, compressed, and stretched helical scaffolds (Figure 5a,b). As expected, the two helices show a strong photostability, inferred from ECD studies that show how the ECD traces remain almost unaltered even after 240 min of irradiation with visible light. This is attributed to the *quasi*-static behavior of the PPA and not to the electronic properties of the sulfoxide group. In literature, it is found that PPAs bearing a sulfoxide group at para position show a *cis*- to *trans*- isomerization of double bonds due to delocalization of radicals generated at the polyene, which can migrate to the sulfoxide group, producing the loss of its chirality.[30]

In addition, thermal stability studies of poly-(*R*)-**1** in $CHCl_3$ and THF reveal also the poor dynamic character of the PPA and its correlated high thermal stability (Figure 5c,d). In both solvents, the ECD trace obtained for poly-(*R*)-**1** is not affected by temperature changes, either by cooling down or heating up the cuvette containing a solution of the polymer. These results indicate that once the polymer is dissolved in a certain solvent, the helical folding is not perturbed by temperature changes.

In conclusion, it has been demonstrated through a rational design that photostability of PPAs is directly related to its dynamic behavior. Thus, those PPAs with a high dynamic behavior, whose helical sense or elongation can be altered by the presence of external stimuli are more prompt to degrade under light exposure due to photoisomerization of the double bonds that end up with a photochemical electrocyclization of the polyene backbone. On the other hand, PPAs with a restricted conformational composition and therefore a poor dynamic behavior shows a great

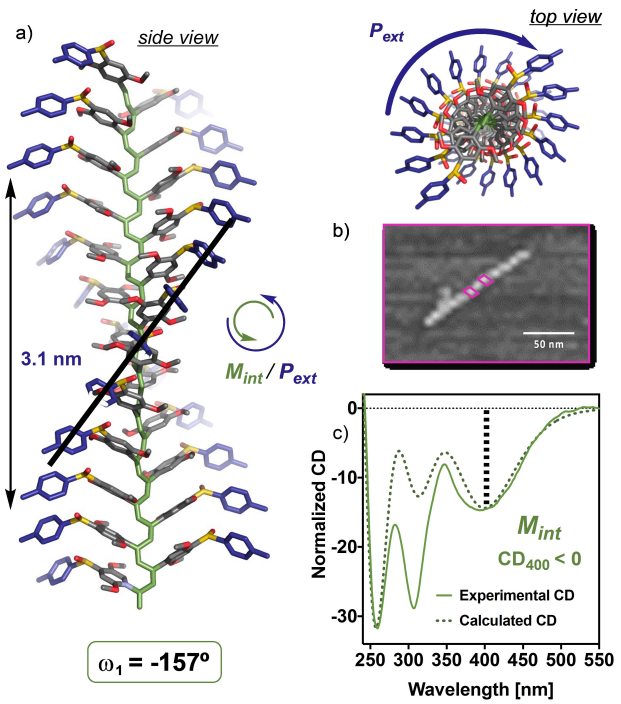

Figure 4. a) 3D structure adopted by poly-(*R*)-**1** in THF. b) AFM image of a 2D crystal of poly-(*R*)-**1** prepared in THF. c) Theoretical and experimental ECD spectra of poly-(*R*)-**1**. [poly-(*R*)-**1**] = 0.3 mg mL^{-1}.

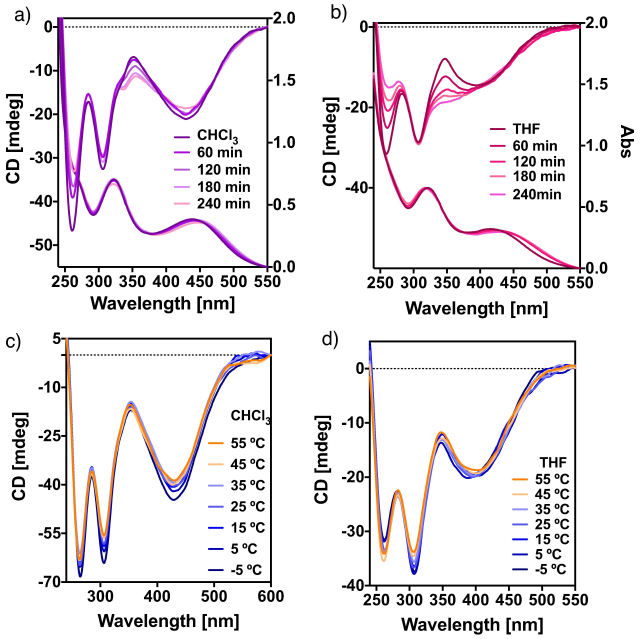

Figure 5. Photostability and thermal stability ECD studies of poly-(*R*)-**1** in a,c) $CHCl_3$ and b,d) THF. [poly-(*R*)-**1**] = 0.3 mg mL^{-1}; irradiation with visible light (350–550 nm).

photostability, being the helical scaffold not affected by irradiation with UV light. Therefore, dynamic behavior and photostability in PPAs are compromised, fact that is necessary to consider in the design and potential application of PPAs.

Acknowledgements

We thank Servicio de Microscopía Electrónica (RIAIDT, USC). Financial support from AEI (PID2019-109733GB-I00), Ministerio de Ciencia e Innovación (PID2019-107307RB-100 and PID2020-117605GB-100, PID2020-113059GB-C21, PID2020-113059GB-C22). Xunta de Galicia (ED431C 2018/30, ED431C 2021/40, Centro Singular de Investigación de Galicia acreditación 2019–2022, ED431G 2019/03 and the European Regional Development Fund (ERDF) is gratefully acknowledged. F.R.T. thanks Xunta de Galicia for a predoctoral contract. We acknowledge CESGA for computational time and we also thank Servicio de Nanotecnología y Análisis de Superficies (CACTI-CINBIO, UVigo).

Conflict of Interest

The authors declare no conflict of interest.

Data Availability Statement

The data that support the findings of this study are available in the supplementary material of this article.

Keywords: Chiroptical Properties · Dynamic Helices · Helical Structure · Photostability · Poly(phenylacetylene)s

[1] E. Yashima, N. Ousaka, D. Taura, K. Shimomura, T. Ikai, K. Maeda, *Chem. Rev.* **2016**, *116*, 13752–13990.
[2] E. Yashima, K. Maeda, H. Iida, Y. Furusho, K. Nagai, *Chem. Rev.* **2009**, *109*, 6102–6211.
[3] T. Nakano, Y. Okamoto, *Chem. Rev.* **2001**, *101*, 4013–4038.
[4] J. Tarrío, R. Rodríguez, B. Fernández, E. Quiñoá, F. Freire, *Angew. Chem. Int. Ed.* **2022**, *61*, e202115070; *Angew. Chem.* **2022**, *134*, e202115070.
[5] E. Schwartz, M. Koepf, H. J. Kitto, R. J. M. Nolte, A. E. Rowan, *Polym. Chem.* **2011**, *2*, 33–47.
[6] E. Yashima, K. Maeda, Y. Furusho, *Acc. Chem. Res.* **2008**, *41*, 1166–1180.
[7] R. Sakai, E. B. Barasa, N. Sakai, S.-I. Sato, T. Satoh, T. Kakuchi, *Macromolecules* **2012**, *45*, 8221–8227.
[8] E. Yashima, K. Maeda, *Macromolecules* **2008**, *41*, 3–12.
[9] K. Maeda, E. Yashima, *Top. Curr. Chem.* **2006**, *265*, 47–88.
[10] R. Nonokawa, E. Yashima, *J. Am. Chem. Soc.* **2003**, *125*, 1278–1283.
[11] E. Yashima, K. Maeda, Y. Okamoto, *Nature* **1999**, *399*, 449–451.
[12] E. Yashima, K. Maeda, T. Matsushima, Y. Okamoto, *Chirality* **1997**, *9*, 593–600.
[13] R. Rodríguez, E. Suárez-Picado, E. Quiñoá, R. Riguera, F. Freire, *Angew. Chem. Int. Ed.* **2020**, *59*, 8616–8622; *Angew. Chem.* **2020**, *132*, 8694–8700.
[14] F. Freire, J. M. Seco, E. Quiñoá, R. Riguera, *J. Am. Chem. Soc.* **2012**, *134*, 19374–19383.
[15] F. Ishiwari, K. Nakazono, Y. Koyama, T. Takata, *Angew. Chem. Int. Ed.* **2017**, *56*, 14858–14862; *Angew. Chem.* **2017**, *129*, 15054–15058.
[16] R. Rodríguez, S. Arias, E. Quiñoá, R. Riguera, F. Freire, *Nanoscale* **2017**, *9*, 17752–17757.
[17] N. Zhu, K. Nakazono, T. Takata, *Chem. Commun.* **2016**, *52*, 3647–3649.
[18] S. Leiras, F. Freire, J. M. Seco, E. Quiñoá, R. Riguera, *Chem. Sci.* **2013**, *4*, 2735–2743.
[19] K. Maeda, H. Mochizuki, M. Watanabe, E. Yashima, *J. Am. Chem. Soc.* **2006**, *128*, 7639–7650.
[20] K. Maeda, N. Kamiya, E. Yashima, *Chem. Eur. J.* **2004**, *10*, 4000–4010.
[21] T. Ikai, R. Ishidate, K. Inoue, K. Kaygisiz, K. Maeda, E. Yashima, *Macromolecules* **2020**, *53*, 973–981.
[22] M. Alzubi, S. Arias, R. Rodríguez, E. Quiñoá, R. Riguera, F. Freire, *Angew. Chem. Int. Ed.* **2019**, *58*, 13365–13369; *Angew. Chem.* **2019**, *131*, 13499–13503.
[23] R. Rodríguez, E. Quiñoá, R. Riguera, F. Freire, *Chem. Mater.* **2018**, *30*, 2493–2497.
[24] T. Van Leeuwen, G. H. Heideman, D. Zhao, S. J. Wezenberg, B. L. Feringa, *Chem. Commun.* **2017**, *53*, 6393–6396.
[25] M. Alzubi, S. Arias, I. Louzao, E. Quiñoá, R. Riguera, F. Freire, *Chem. Commun.* **2017**, *53*, 8573–8576.
[26] S. Arias, F. Freire, E. Quiñoá, R. Riguera, *Polym. Chem.* **2015**, *6*, 4725–4733.
[27] F. Freire, J. M. Seco, E. Quiñoá, R. Riguera, *Angew. Chem. Int. Ed.* **2011**, *50*, 11692–11696; *Angew. Chem.* **2011**, *123*, 11896–11900.
[28] I. Louzao, J. M. Seco, E. Quiñoá, R. Riguera, *Angew. Chem. Int. Ed.* **2010**, *49*, 1430–1433; *Angew. Chem.* **2010**, *122*, 1472–1475.
[29] S. Arias, J. Bergueiro, F. Freire, E. Quiñoá, R. Riguera, *Small* **2016**, *12*, 238–244.
[30] K. Huang, S. Y. Mawatary, A. Miyasaka, Y. Sadahiro, M. Tabata, Y. Kashiwaya, *Polymer* **2007**, *48*, 6366–6373.
[31] S. Arias, M. Núñez-Martínez, E. Quiñoá, R. Riguera, F. Freire Polym, *Chem* **2017**, *8*, 3740–3745.
[32] M. Núñez-Martínez, S. Arias, E. Quiñoá, R. Riguera, F. Freire, *Chem. Mater.* **2021**, *33*, 4805–481.
[33] K. Maeda, K. Morino, Y. Okamoto, T. Sato, E. Yashima, *J. Am. Chem. Soc.* **2004**, *126*, 4329–4342.
[34] S. Li, K. Liu, G. Kuang, T. Masuda, A. Zhang, *Macromolecules* **2014**, *47*, 3288–3296.
[35] S. Arias, F. Freire, M. Calderón, J. Bergueiro, *Angew. Chem. Int. Ed.* **2017**, *56*, 11420–11425; *Angew. Chem.* **2017**, *129*, 11578–11583.
[36] F. Wang, C. Zhou, K. Liu, J. Yan, W. Li, T. Masuda, A. Zhang, *Macromolecules* **2019**, *52*, 8631–8642.
[37] J. Bergueiro, M. Núñez-Martínez, S. Arias, E. Quiñoá, R. Riguera, F. Freire, *Nanoscale Horiz.* **2020**, *5*, 495–500.
[38] R. Rodríguez, E. Suárez-Picado, E. Quiñoá, R. Riguera, F. Freire, *Angew. Chem. Int. Ed.* **2020**, *59*, 8616–8622; *Angew. Chem.* **2020**, *132*, 8694–8700.
[39] K. Cobos, R. Rodriguez, O. Domarco, B. Fernandez, E. Quinoa, R. Riguera, R. F. Freire, *Macromolecules* **2020**, *53*, 3182–3193.
[40] E. Suárez-Picado, E. Quiñoá, R. Riguera, F. Freire, *Angew. Chem. Int. Ed.* **2020**, *59*, 4537–4543; *Angew. Chem.* **2020**, *132*, 4567–4573.

[41] M. Fukuda, R. Rodríguez, Z. Fernández, T. Nishimura, D. Hirose, G. Watanabe, E. Quiñoá, F. Freire, K. Maeda, *Chem. Commun.* **2019**, *55*, 7906–7909.
[42] K. Maeda, M. Ishikawa, E. Yashima, *J. Am. Chem. Soc.* **2004**, *126*, 15161–15166.
[43] Y. Cao, L. Ren, Y. Zhang, X. Lu, X. Zhang, J. Yan, W. Li, T. Masuda, A. Zhang, *Macromolecules* **2021**, *54*, 7621–7631.
[44] S. Leiras, E. Suárez-Picado, E. Quiñoá, R. Riguera, F. Freire, *Giant* **2021**, *7*, 100068.
[45] R. Ishidate, T. Sato, T. Ikai, S. Kanoh, E. Yashima, K. Maeda, *Polym. Chem.* **2019**, *10*, 6260–6268.
[46] D. Hirose, A. Isobe, E. Quiñoá, F. Freire, K. Maeda, E. Yashima, K. Maeda, *J. Am. Chem. Soc.* **2019**, *141*, 8592–8598.
[47] Y. Zhou, C. Zhang, Q. Geng, L. Liu, H. Dong, T. Satoh, Y. Okamoto, *Polym. J.* **2017**, *131*, 17–24.
[48] Y. Zhou, C. Zhang, Z. Zhou, R. Zhu, L. Liu, J. Bai, H. Dong, T. Satoh, Y. Okamoto, *Polym. Chem.* **2019**, *10*, 4810–4817.
[49] M. Ando, R. Ishidate, T. Ikai, K. Maeda, E. Yashima, *J. Polym. Sci. Part A* **2019**, *57*, 2481–2490.
[50] C. Zhang, Y. Qiu, S. Bo, F. Wang, Y. Wang, L. Liu, Y. Zhou, H. Niu, H. Dong, T. Satoh, *J. Polym. Sci. Part A* **2019**, *57*, 1024–1031.
[51] Z. Tang, H. Iida, H. Y. Hu, E. Yashima, *ACS Macro Lett.* **2012**, *1*, 261–265.
[52] H. Iida, Z. Tang, E. Yashima, *J. Polym. Sci. Part A* **2013**, *51*, 2869–2879.
[53] S. A. Karim, R. Nomura, T. Masuda, *J. Polym. Sci. Part A* **2001**, *39*, 3130–3136.
[54] V. Percec, J. G. Rudick, P. Nombel, W. Buchowicz, *J. Polym. Sci. Part A* **2002**, *40*, 3212–3220.
[55] V. Percec, J. G. Rudick, *Macromolecules* **2005**, *38*, 7241–7250.
[56] L. Liu, T. Namikoshi, Y. Zang, T. Aoki, S. Hadano, Y. Abe, I. Wasuzu, T. Tsutsuba, M. Teraguchi, T. Kaneko, *J. Am. Chem. Soc.* **2013**, *135*, 602–605.
[57] Y. Tang, L. Liu, J. Suzuki, M. Teraguchi, T. Kaneko, T. Aoki, *Chirality* **2022**, *34*, 450–461.
[58] F. Rey-Tarrío, R. Rodríguez, E. Quiñoá, R. Riguera, F. Freire, *Angew. Chem. Int. Ed.* **2021**, *60*, 8095–8103; *Angew. Chem.* **2021**, *133*, 8176–8184.
[59] S. Resa, D. Miguel, S. Guisán-Ceinos, G. Mazzeo, D. Choquesillo-Lazarte, S. Abbate, L. Crovetto, D. J. Cárdenas, M. C. Carreño, M. Ribagorda, G. Longhi, A. J. Mota, L. Á. de Cienfuegos, J. M. Cuerva, *Chem. Eur. J.* **2018**, *24*, 2653–2662.
[60] P. Reiné, A. M. Ortuño, S. Resa, L. Á. de Cienfuegos, V. Blanco, M. J. Ruedas-Rama, G. Mazzeo, S. Abbate, A. Lucotti, M. Tommasini, S. Guisán-Ceinos, M. Ribagorda, A. G. Campaña, A. Motta, G. Longhi, D. Miguel, J. M. Cuerva, *Chem. Commun.* **2018**, *54*, 13985–13988.
[61] S. Resa, P. Reiné, L. Á. de Cienfuegos, S. Guisán-Ceinos, M. Ribagorda, G. Longhi, G. Mazzeo, S. Abbate, A. J. Mota, D. Miguel, J. M. Cuerva, *Org. Biomol. Chem.* **2019**, *17*, 8425–8434.
[62] M. C. Carreño, I. García, I. Núñez, E. Merino, M. Ribagorda, S. Pieraccini, G. P. Spada, *J. Am. Chem. Soc.* **2007**, *129*, 7089–7100.
[63] Deposition Number 2174549 contains the supplementary crystallographic data for this paper. These data are provided free of charge by the joint Cambridge Crystallographic Data Centre and Fachinformationszentrum Karlsruhe Access Structures service.
[64] V. Percec, M. Peterca, J. G. Rudick, E. Aqad, M. R. Imam, P. A. Heiney, *Chem. Eur. J.* **2007**, *13*, 9572–9581.
[65] R. Rodríguez, E. Quiñoá, R. Riguera, F. Freire, *Small* **2019**, *15*, 1805413.
[66] R. Rodríguez, E. Quiñoá, R. Riguera, F. Freire, *J. Am. Chem. Soc.* **2016**, *138*, 9620–9628.
[67] J. Kumaki, S. I. Sakurai, E. Yashima, *Chem. Soc. Rev.* **2009**, *38*, 737–746.

Manuscript received: May 24, 2022
Accepted manuscript online: June 22, 2022
Version of record online: July 8, 2022